

# Dehydration kinetics of muscovite by in situ infrared microspectroscopy

Kazuyo Tokiwai · Satoru Nakashima

Received: 5 March 2009 / Accepted: 8 May 2009 / Published online: 26 May 2009  
© Springer-Verlag 2009

**Abstract** Dehydration behavior of muscovite flake was investigated at 760–860°C by using in situ high-temperature IR microspectroscopy for the OH absorption band around 3,620 cm<sup>-1</sup>. Isothermal kinetic heating experiments at each temperature gave detailed decrease curves of the OH band area with time. These curves have been simulated by the first and second order reactions or mono- and two-dimensional diffusion processes. The mono-dimensional diffusion was found to give the best fit to the experimental data and apparent diffusion coefficients  $D$  were determined at 760–860°C with the activation energy of  $290 \pm 20$  kJ/mol. The apparent diffusion coefficients  $D$  varied with the sample thickness  $L$ . This variation can be explained by an  $m$  layers model with a unit length of  $L'$  with a constant diffusion coefficient  $D'$ . Therefore, the dehydration process might be rate-limited by mono-dimensional diffusion through tetrahedral silicate sheet perpendicular to (001) planes of muscovite with a unit length of  $L'$ .

**Keywords** Muscovite · OH · In situ IR microspectroscopy · Dehydration · Kinetics · Diffusion

## Introduction

Dehydration of hydrous minerals is one of the important elementary steps in the earth. For example, sedimentary geological formations containing abundant hydrous

minerals accumulating at the earth's surface are introduced to the earth's interior by the plate subduction processes. At higher temperatures and pressures, hydrous minerals become unstable and are transformed into anhydrous minerals (Fyfe et al. 1978). This transformation from hydrous to anhydrous minerals in the earth's interior includes dehydration processes of hydrous minerals. Since rates of mineralogical and geological processes are controlled primarily by the slowest elementary step among the operating processes, detailed knowledge of rate-determining step for the dehydration process of hydrous minerals is essential.

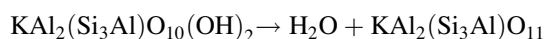
Muscovite was selected here as a representative hydrous mineral containing structural OH. The structure of muscovite [ideally  $\text{KAl}_2(\text{OH})_2(\text{Si}_3\text{Al})\text{O}_{10}$ ] can be described in terms of an Al-centered octahedral sheet sandwiched between two (Si, Al)-centered tetrahedral sheets so that the layer unit is a true mica 2:1 sheet whose overall charge is compensated by K cations in the inter-sheet region (Brindley and Brown 1980; Bailey 1984). In the octahedral sheet, only two out of three Al sites are occupied (labeled as M2 sites) inducing a relaxation of the framework around the vacant site (labeled M1). The apical 6-ring of tetrahedra displays a ditrigonal distortion in order to allow the fit between the tetrahedral and the octahedral sheets of the layer unit (Toraya 1981).

In previous works, muscovite dehydration was mainly studied by X-ray diffractometry (Eberhart 1963; Udagawa et al. 1973, 1974; Guggenheim et al. 1987; Mazzucato et al. 1999), thermogravimetric (TG) and differential thermal analyses (DTA) (Holt et al. 1958, 1964; Kodama and Brydon 1968; Hanykyr et al. 1985; Gridi-Bennadji and Blanchart 2007), energy calculation (Abbott 1994) and IR spectroscopy (Gaines and Vedder 1964; Rouxhet 1970; Shishelova et al. 1974; Aines and Rossman 1985). X-ray

K. Tokiwai · S. Nakashima (✉)  
Department of Earth and Space Science,  
Osaka University, 1-1 Machikaneyama-cho,  
Toyonaka, Osaka 560-0043, Japan  
e-mail: satoru@ess.sci.osaka-u.ac.jp

diffraction has been mainly used to investigate muscovite structures and phase transitions. IR spectroscopy was used to study structural characteristics of hydroxyls from OH peak forms at high temperatures. These structural studies have always been carried out separately from the kinetic studies. On the other hand, TG and DTA were used to investigate the kinetics of muscovite dehydration.

The dehydration reaction is chemically very simple:



and it involves condensation of two hydroxyl groups to form a water molecule.

Eberhart (1963) observed a spinel-like phase forming above 1,050°C. A structural model for the dehydroxylated phase has been proposed on the basis of single crystal diffraction data by Udagawa et al. (1974): the Al atoms switch from 6 to 5 coordination and have a very short bonding distance (1.69 Å) to the oxygen atom shared by two Al atoms, which is considerably charge undersaturated (Guggenheim et al. 1987).

Concerning the kinetics of muscovite dehydration, there are many published data which cover a wide range of temperatures and forms (e.g., Sabatier 1955; Eberhart 1963; Holt et al. 1958, 1964; Gaines and Vedder 1964; Kodama and Brydon 1968; Hanykyr et al. 1985; Mazzucato et al. 1999; Gridi-Bennadji and Blanchart 2007). These were studied by different methods and different rate-limiting steps have been proposed. The diffusion process has been recently suggested to be the rate-limiting step, albeit the detailed conclusions differ, especially concerning the dimensionality of the diffusion mechanism, and the physical interpretation of the process (Mazzucato et al. 1999).

Mazzucato et al. (1999) considered that the reaction of muscovite dehydration is a multi-step process including (a) the early condensation of two adjacent hydroxyls in the octahedral sheet to form a water molecule; (b) the one-dimensional diffusion of the water molecule through the 6-ring of the tetrahedral sheet, and (c) the diffusion of the water molecule in the inter-sheet region to reach the surface of the crystallite.

Holt et al. (1958, 1964) measured dehydration of muscovite by thermogravimetry (TG) and the dehydration mechanism was considered to be the simple first order reaction. The activation energy was 377 kJ/mol. Hanykyr et al. (1985) also considered the simple first order reaction for TG results on muscovite. They assumed sizes of mica plates are the same and the activation energy was 489–517 kJ/mol.

Kodama and Brydon (1968) also studied muscovite dehydration by TG (powder) and the process was considered to be two-dimensional diffusion in vacuum. The activation energy was 226 kJ/mol. Rouxhet (1970) made a

hypothesis that the diffusion pathway was one-dimensional along the  $c^*$  axis. The obtained activation energy for diffusion and deuteration in a muscovite mica by IR spectroscopy was 197 kJ/mol.

Mazzucato et al. (1999) studied muscovite dehydration by in situ high-temperature X-ray powder diffraction (XRPD). They considered that the nucleation of dehydroxylated phase was followed by the growth of a high-temperature muscovite phase where most of Al ions were fivefold coordinated. The kinetic analysis of their data using an Avrami-type model yields values for the reaction order compatible with a reaction mechanism limited by a one-dimensional diffusion step. Apparent activation energy was about 251 kJ/mol. Gridi-bennadji and Blanchart (2007) conducted isothermal TG measurements using large muscovite flakes and analyzed the data with the Avrami theory. The activation energy was 190–214 kJ/mol. They reported that Mazzucato et al. (1999) did not consider multiple steps occurring during successive stages and the obtained activation energy value was only an average value of the multiple stages.

Considering these previous works, it is important to consider the sample forms either in powders or in flakes. Although dehydration of muscovite is primarily related to OH decrease, the nucleation of the dehydroxylated phase is mainly considered in the previous works. Therefore, the aims of this study are to directly observe OH in muscovite using in situ infrared spectroscopy and to investigate dehydration mechanism of the muscovite in the form of not in powders but in flakes close to natural systems.

## Starting materials

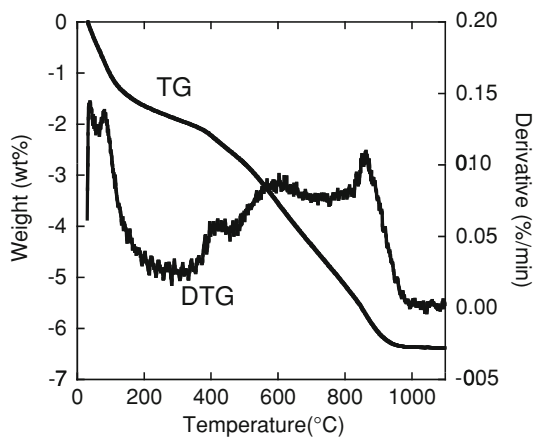
### Sample characterization

The starting material used in this study is muscovite-2M<sub>1</sub> from Ishikawa, Fukushima, Japan. The chemical compositions of muscovite were analyzed with a JEOL-JXA-8800M electron microprobe using a defocused beam (10 μm in diameter), 15 kV accelerating voltage, and 12-nA beam current. The analytical results are listed in Table 1.

The water content of the sample was determined by thermal analyses. Thermogravimetry (TG) was carried out on the sample powder using a SII TG/DTA 6000 instrument from 23 to 1,100°C with a heating rate of 10°C/min (Fig. 1). The TG curve in Fig. 1 shows a weight loss of about 2% until about 200°C, which may be attributed to adsorbed water (Guggenheim et al. 1987). The weight loss in the range from 200 to 950°C is  $4.46 \pm 0.24$  wt.%. Thus, the water content of muscovite was determined to be

**Table 1** Chemical composition of the muscovite sample

Oxide	Wt.%
SiO <sub>2</sub>	46.43
TiO <sub>2</sub>	0.03
Al <sub>2</sub> O <sub>3</sub>	35.48
Cr <sub>2</sub> O <sub>3</sub>	0.01
FeO	2.78
MnO	0.02
MgO	0.15
NiO	0.01
CaO	0.00
Na <sub>2</sub> O	0.78
K <sub>2</sub> O	10.04
Total	95.73

**Fig. 1** Thermogravimetry (TG) and its differential (DTG) curves for the muscovite sample at a heating rate of 10°C/min

$4.46 \pm 0.24$  wt.% which is consistent with the total weight percents of 95.73 wt.% by the EPMA analysis (Table 1). Based on the chemical compositions in Table 1 and the water contents, the structural formula of this sample can be expressed as:



The obtained chemical and mineralogical compositions are very close to ideal compositions  $(\text{KAl}_2(\text{Si}_3\text{Al})\text{O}_{10}(\text{OH})_2)$  of muscovite (Bailey 1984).

#### Sample preparation

Thin flakes of the muscovite sample were separated from the aggregates with tweezers by using perfect cleavage (001) planes. These muscovite flakes were cut with a punch into circular plates of about 3 mm in diameter.

The thicknesses of the samples were measured with a Laser Scanning Confocal Microscope (LSCM) (KEYENCE, Color Laser 3D Profile Microscope VK-8500, and VK-8510) (Okumura et al. 2003). The LSCM measurements were carried out at the positions analyzed by FT-IR microspectroscopy. The refractive index of muscovite (1.60; Klein and Hurlbut Jr 1993) was used to determine the sample thickness based on the LSCM data.

#### Experimental methods

Dehydration experiments at 760–860°C were conducted using a Linkam TS1500 heating stage under a Fourier transform infrared (FT-IR) microscope (Jasco IRT30 + FTIR620: MCT detector, ceramic IR source, and KBr beam splitter) (e.g., Okumura and Nakashima 2005). Circular muscovite plates [about 3 mm in diameter, parallel to the (001) crystallographic planes] having the thickness of about 8 μm were used for IR measurements. Table 2 lists experimental conditions.

The in situ heating experiments on these muscovite flake samples were conducted after Okumura and Nakashima (2006). First, the temperature of the heating stage was elevated at a rate of 100°C/min and held at a desired temperature. Second, at the desired temperature a transmission spectrum of the sapphire plate on the heating stage was measured by the FT-IR microspectrometer as a

**Table 2** Experimental conditions for the muscovite dehydration

Sample name	Experimental temperature (°C)	Sample thickness (μm)	Thickness error (μm)	Preparation time (s)	Heating time (h)
081014a-7	760	8.6	0.70	40	12
081014a-10	790	8.7	3.5	50	12
081014a-5	800	9.3	0.2	60	4
081014a-2	810	9.0	1.3	60	3
081014b-6	820	7.9	0.2	40	3
081014b-1	840	8.8	1.2	40	3
081014a-1	860	8.0	0.2	40	2

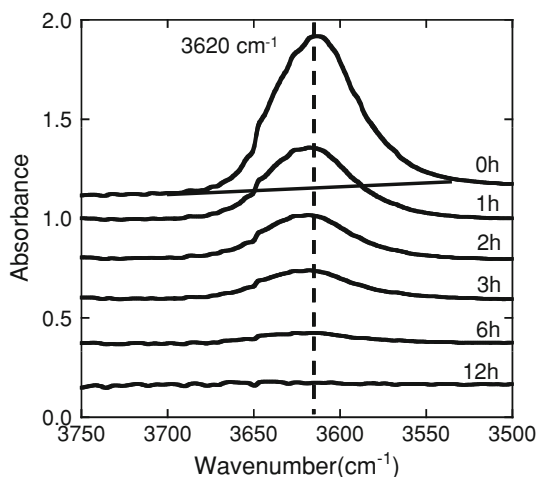


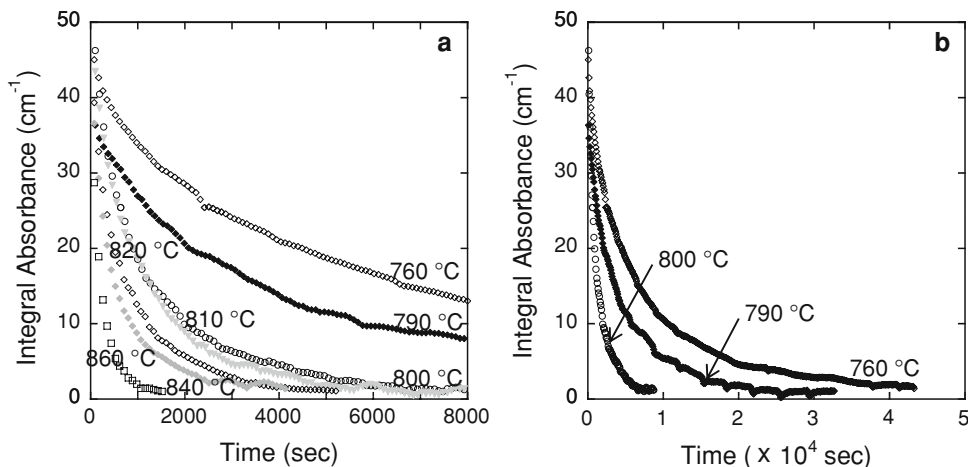
**Fig. 2** Changes with time of OH absorption band around  $3,620\text{ cm}^{-1}$  during in situ heating experiments of muscovite at  $760^\circ\text{C}$

background spectrum. Finally, a sample thin flake was put on the sapphire plate on the heating stage and the sample measurement by the FT-IR microspectrometer was started just after the sample setting. An IR spectrum was obtained by co-adding spectra of 100 scans with an unpolarized infrared beam. The sample measurement was repeated at a 90-s interval using an interval measurement program. Since 100 scans took 80 s, the IR spectra represent the average for 80 s. The starting time of the experiment was taken at the time when a sample was put on the sapphire plate on the heating stage, because some water of muscovite could have been already dehydrated during the sample setting. All the spectra in this study were obtained by the rectangular aperture size of  $100 \times 100\ \mu\text{m}$ .

## Results

A typical series of spectral change of muscovite during the in situ heating experiments is shown in Fig. 2 at  $760^\circ\text{C}$  for

**Fig. 3** Changes with time in integral absorbance (band area) of OH in muscovite. **a** Data for all the temperatures for a short time period; **b** data for a longer time period at 760, 790 and  $800^\circ\text{C}$



0–12 h. The absorption band around  $3,620\text{ cm}^{-1}$  is assigned to stretching vibration of OH (Gaines and Vedder 1964; Rossman 1984; Aines and Rossman 1985). The intensity of the  $3,620\text{ cm}^{-1}$  band decreased with time, which indicated that OH in muscovite decreased during the dehydration experiment. To describe quantitatively the OH decrease, we measured integral intensity (absorbance) from  $3,540$  to  $3,700\text{ cm}^{-1}$  with a straight baseline correction (Fig. 2).

Changes with time in measured band areas (integral absorbances) of the  $3,620\text{ cm}^{-1}$  band at 760, 790, 800, 810, 820, 840 and  $860^\circ\text{C}$  are shown in Fig. 3. As is stated above, initial integral intensities in the experiments were assumed to be the first values at the each temperature obtained at 40 s after starting the dehydration experiments, because an IR measurement with 100 scans took about 80 s and the spectra were considered to represent the average during the 80 s of measurement. The maximum error of integral absorbance of the  $3,620\text{ cm}^{-1}$  band was estimated to be  $\pm 0.16$ , because the peak area was determined by integrating peak height with the error of  $\pm 0.001$  from  $3,540$ – $3,700\text{ cm}^{-1}$  (Okumura and Nakashima 2004). The error of the peak height ( $\pm 0.001$ ) is estimated from the noise level of the background spectrum.

## Reaction kinetics

Experimental results (Fig. 3) show that the content of OH in muscovite decreased with time during heating from 760 to  $860^\circ\text{C}$ .

The reaction of muscovite dehydration is considered to be a multi-step process including (Mazzucato et al. 1999):

- The early condensation of two adjacent hydroxyls in the octahedral sheet to form a water molecule;
- The mono-dimensional diffusion of the water molecule through the 6-ring of the tetrahedral sheet, that is the actual escape window to the inter-sheet space;

c. The diffusion of the water molecule in the inter-sheet region to reach the surface of the crystallite.

The following kinetic rate laws can be considered.

1. The first order reaction.

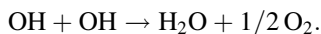
OH in muscovite decrease rate is in proportion to the concentration of OH in muscovite. This first order reaction follows the formula:

$$[A] = [A]_0 \exp(-kt), \quad \text{or} \quad \ln[A] = \ln[A]_0 - kt, \quad (1)$$

where  $[A]$  is the absorbance;  $[A]_0$  is the initial absorbance;  $k$  is the first order reaction rate constant  $[s^{-1}]$ ; and  $t$  is the time  $[s]$ .

2. The second order reaction.

If the rate-determining reaction is the above (a) step, two OH in muscovite react together to form a  $H_2O$  molecule following the second order reaction:



The rate law for the second order reaction is

$$\frac{1}{[A]} = \frac{1}{a} + kt, \quad (2)$$

where  $[A]$  is the absorbance;  $a$  is a constant;  $k$  is the second order reaction rate constant  $(s^{-1})$ ; and  $t$  is the time  $(s)$ .

3. The mono-dimensional diffusion-limited reaction.

If the mono-dimensional diffusion of  $H_2O$  through the 6-ring of the tetrahedral sheet [the above (b) step] is the rate-determining process, the OH decrease can be expressed by the following diffusion equation.

Assuming that muscovite flakes used in this study are considered to be plane sheets and the water concentration at their surfaces remains zero, the diffusion-out rate from the plane sheet can be written as (Carslaw and Jaeger 1959):

$$M_t = M \times \sum_{n=0}^{\infty} \left\{ \frac{8}{(2n+1)^2 \pi^2} \right\} \cdot \exp \left\{ \frac{-D(2n+1)^2 \pi^2 t}{L^2} \right\}, \quad (3)$$

where  $M$  is the initial amount of water in a sample;  $M_t$  is the amount of water in a sample at the time  $t$ ;  $D$  is the diffusivity;  $t$  is the time;  $L$  is the sample thickness. Figure 4 shows the schematic diagram of the boundary and the geometry of the diffusion experiments.

4. The two-dimensional diffusion-limited reaction.

If the two-dimensional diffusion of  $H_2O$  in the inter-sheet region [the above (c) step] is the rate-determining process, we can consider the following diffusion-out rate from a circular cylinder (Carslaw and Jaeger 1959),

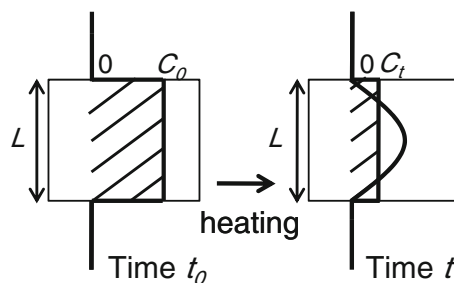


**Fig. 4** Schematic models for mono-dimensional diffusion from a plane sheet with a thickness of  $L$  and initial concentration of  $C_0$ . After a time  $t$ , the concentration decreases to  $C_t$  by the diffusion. The  $C_t$  value is indicated as a rectangular area which is equal to the area under the diffusion profile

because the small center areas ( $100 \times 100 \mu m$ ) of circular flake samples ( $3 \text{ mm } \phi$ ) were measured:

$$M_t = M \times \frac{2}{a} \sum_{n=1}^{\infty} \left( \frac{J_0(0)}{\alpha_n J_1(\alpha_n a)} \right) \cdot \exp(-D \alpha_n^2 t), \quad (4)$$

where  $M$  is the initial amount of water in the sample;  $M_t$  is the amount of water in a sample at the time  $t$ ;  $D$  is the diffusivity;  $t$  is the time;  $a$  is the cylinder radius;  $J_0(x)$  is the first type zeroth-order Bessel function;  $J_1(x)$  is the first type first order Bessel function;  $\alpha_n a$  is the root of the first type zeroth-order Bessel function.

The experimental decrease curves (Fig. 3) were fitted by each of the four above hypothesized reactions.

If the experimental results follow (1) the first order reaction, natural logarithm of integral absorbance (y-axis) plotted against time (x-axis) should show a linear decrease based on Eq. 1. However, the experimental data are not linear at each temperature (Fig. 5). Therefore, the present dehydration behavior is not considered to follow the first order reaction.

In (2) the second order reaction (Eq. 2), the inverse of integral absorbance should be proportional to the time. The experimental data are not linear in this plot indicating that the second order reaction is not the rate-limiting step (Fig. 6).

In the diffusion equations (Eqs. 3, 4), the integral absorbance  $M_t$  decreases with the time  $t$ . Initial integral absorbance  $M_0$  is not known, because the sample has already dehydrated to some extent during about 80 s from the sample setting on the heating stage until the middle of the IR measurement, which is taken as the  $t = 0$ . Thus, the initial integral absorbance  $M_0$  is an unknown parameter as well as the diffusion coefficient  $D$ . The values of  $M_0$  and  $D$  were therefore determined by fitting IR data sets by the above equations.

The experimental curves of integral absorbance  $M_t$  at  $760\text{--}860^\circ C$  (Fig. 3) were fitted by the mono-dimensional diffusion equation (Eq. 3) (Fig. 7). The fitting of the

**Fig. 5** Changes with time in natural logarithm of integral absorbance (band area) of OH in muscovite. **a** Data for all the temperatures for a short time period; **b** data for a longer time period at 760, 790 and 800°C

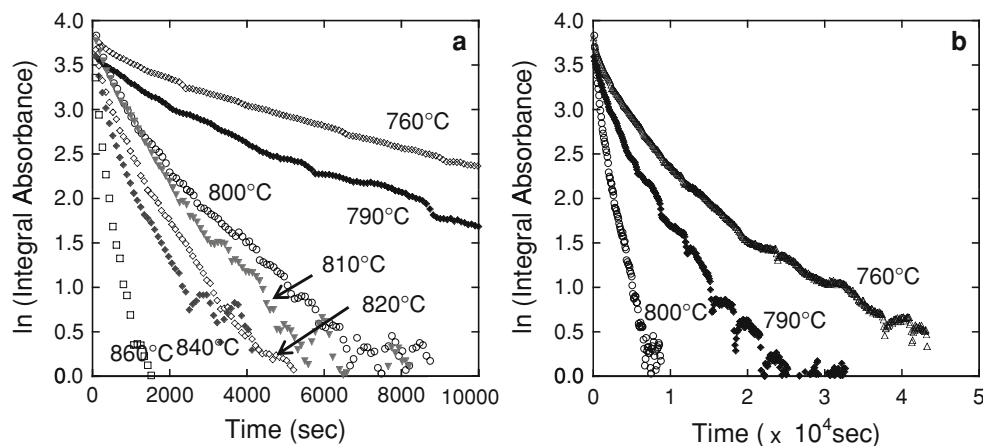
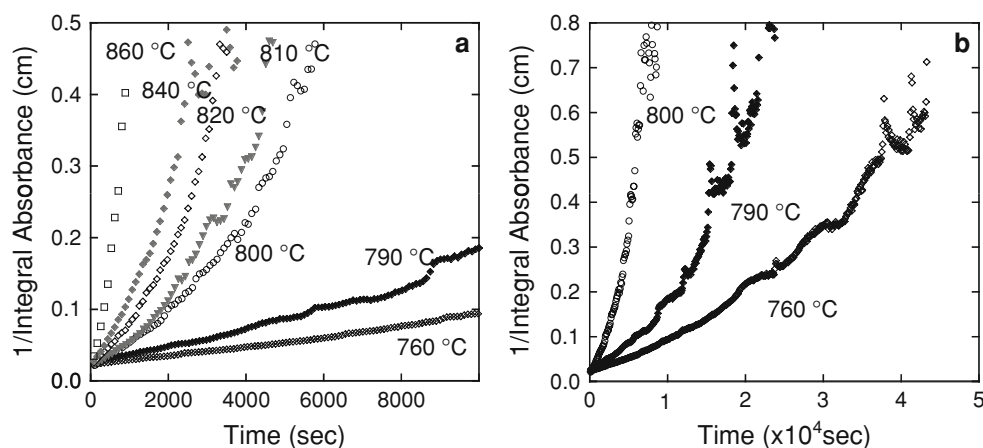


**Fig. 6** Changes with time in the inverse of integral absorbance (band area) of OH in muscovite. **a** Data for all the temperatures for a short time period; **b** data for a longer time period at 760, 790 and 800°C



experimental results show a very good match with the mono-dimensional diffusion process.

The experimental curves  $M_t$  at 760–860°C (Fig. 3) were finally fitted by the two-dimensional diffusion equation (Eq. 4) (Fig. 8). The decrease curves cannot be reproduced by the two-dimensional diffusion equation, especially for the early stage. Therefore, the two-dimensional diffusion cannot explain the experimental results.

Based on the above fitting results, the mono-dimensional diffusion was found to be the best fit among the rate laws tested.

#### Arrhenius plots

All the experimental results of muscovite dehydration were fitted by the mono-dimensional diffusion equation (Eq. 3) to obtain diffusion coefficients  $D$  at 760–860°C (Fig. 7). These data are now plotted in an Arrhenius diagram (Fig. 9). Obtained diffusion coefficients show a linear trend in this diagram following the Arrhenius equation:

$$D = D_0 \exp(-E_a/RT), \quad (5)$$

where  $E_a$  denotes the activation energy (kJ/mol);  $R$  is the gas constant (8.31 J/K mol); and  $T$  is the absolute temperature (K). The fitting of the experimental data by the above Arrhenius equation gives the activation energy  $E_a$  value of  $290 \pm 20$  kJ/mol and  $D_0 = 0.92$  m<sup>2</sup>/s (Fig. 9). The obtained  $E_a$  value is in the same order as the value reported by Mazzucato et al. (1999) for muscovite dehydration analyzed by the mono-dimensional diffusion ( $E_a = 251$  kJ/mol).

#### Discussion

Dehydration rates of muscovite at 760–860°C have been determined from changes with time in the band area at  $3,620$  cm<sup>-1</sup> due to OH in muscovite. In the determination of the dehydration, the sample thin flakes (about 8 μm in thickness and 3 mmφ circle in size) are assumed to be plane sheets in which water diffuses to only one direction which is perpendicular to flake surface (mono-dimensional diffusion), and the concentrations at sample surfaces are

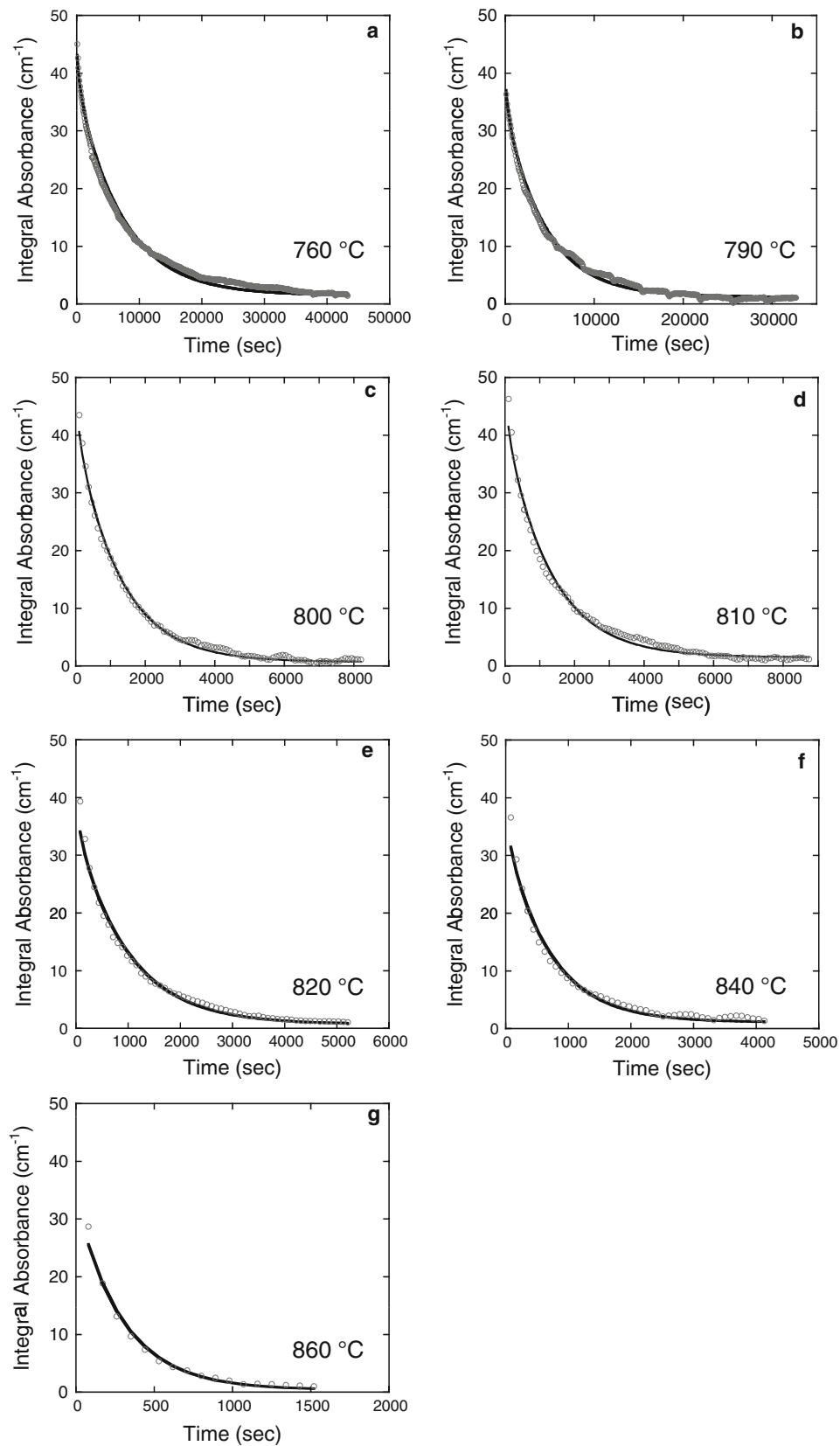


**Fig. 7** Changes with time in integral absorbance (band area) of OH in muscovite at 760 (a), 790 (b), 800 (c), 810 (d), 820 (e), 840 (f) and 860°C (g), fitted by the mono-dimensional diffusion equations at each temperature (black curves)

**Fig. 8** Changes with time in integral absorbance (band area) of OH in muscovite. **a** Data for a short time period at 810, 820, 840 and 860°C, **b** Data for a longer time period at 760, 790 and 800°C, fitted by the two-dimensional diffusion equations at each temperature (black curves)

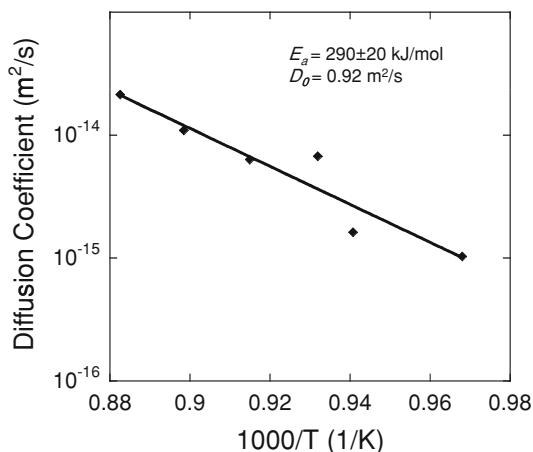
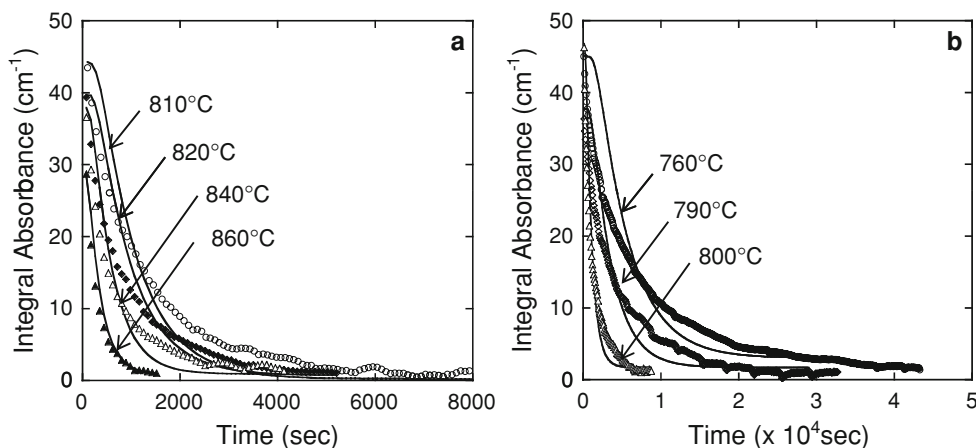


**Fig. 9** Diffusion coefficients  $D$  determined by the mono-dimensional diffusion model for OH in muscovite, plotted in an Arrhenius diagram. The fitting of the data by the Arrhenius equation gives activation energy  $E_a$  of  $290 \pm 20$  kJ/mol and  $D_0$  of  $0.92$  m<sup>2</sup>/s

assumed to be zero (Fig. 4; Eq. 3). Based on this model, even if we change the sample thickness  $L$  in Eq. 3, we should retrieve the same diffusion coefficient  $D$ . Therefore, in the following section, we will test the above hypothesis by changing the sample thickness.

Muscovite flakes with varying thickness from 4.0 to 19.7  $\mu\text{m}$  were prepared by cleaving the flakes (Table 3). The maximum sample thickness was limited to about 20  $\mu\text{m}$  by the saturation of the OH peak at  $3,620$  cm<sup>-1</sup>. These samples were measured by the in situ IR micro-spectroscopy for obtaining changes with time of OH peak area ( $M_t$ ) every 90 s at 840°C. The obtained results were fitted by Eq. 3 with different sample thickness  $L$  to determine diffusion coefficients  $D$  (Fig. 10). The diffusion coefficients  $D$  were plotted against the sample thickness  $L$  in Fig. 11.

The obtained diffusion coefficients  $D$  tend to be larger for increasing sample thickness (Fig. 11). This is in

**Table 3** Experimental conditions of muscovite dehydration at 840°C with varying sample thickness

Sample name	Sample thickness ( $\mu\text{m}$ )	Thickness error ( $\mu\text{m}$ )	Preparation time (s)	Heating time (h)
081014b-5	4.0	0.6	40	2
081014b-2	6.7	1.4	50	2
081014b-1	8.8	1.2	40	3
071112(9)	10.4	1.6	54	1
071109(6)	12.2	2.5	36	2
071109(5)	19.7	2.8	40	10

contradiction to the above mono-dimensional diffusion model. Therefore, other diffusion models should be considered. One possible model is the same type of the mono-dimensional diffusion model within layers of a constant unit length  $L'$  stacking vertically until  $m$  layers separated by other layers without any OH (zero concentration) (Fig. 12). Although it is difficult to find suitable example textures in natural muscovite, we assume here for simplicity of the model that the muscovite layers are separated by other layers without OH. Based on this  $m$  layers model with a unit length of  $L'$  with a constant mono-dimensional diffusion coefficient  $D'$ , the following equation can be applied:

$$M_t = m \times M' \times \sum_{n=0}^{\infty} \left\{ \frac{8}{(2n+1)^2 \pi^2} \right\} \cdot \exp \left\{ \frac{-D'(2n+1)^2 \pi^2 t}{L'^2} \right\}, \quad (6)$$

where  $m \cdot M'$  is the initial amount of water in a sample;  $M_t$  is the amount of water in a sample at the time  $t$ ;  $m$  is a number of layers;  $D'$  is the diffusivity;  $t$  is the time;  $L'$  is the unit length.

Since the  $M_t$  term of the Eqs. 3 and 6 should be equal,  $D/L^2 = D'/L'^2$ , the following relation is hold;



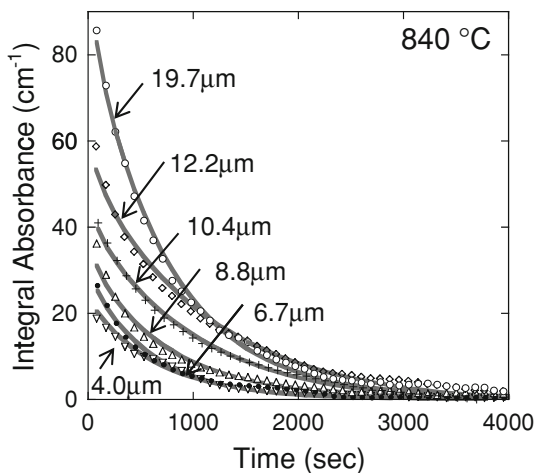


**Fig. 10** Changes with time in integral absorbance (band area) of OH in muscovite during in situ heating experiments at 840°C for flakes of 4.0–19.7 μm thick, fitted by the mono-dimensional diffusion equations at each thickness (gray curves)

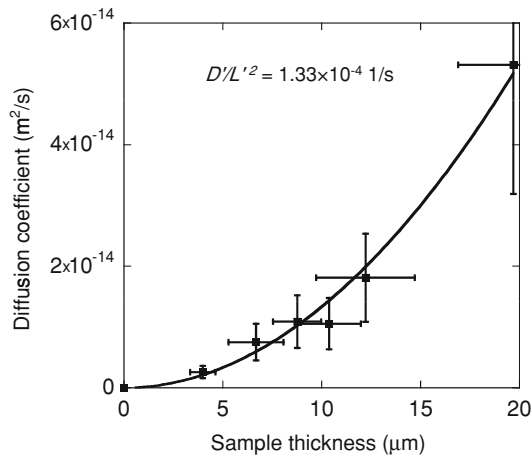


**Fig. 11** Mono-dimensional diffusion coefficients at 840°C for muscovite flakes with varying thickness from 4.0 to 19.7 μm, fitted by the *m* layers model with a unit length of *L'* with a constant mono-dimensional diffusion coefficient *D'* (Fig. 12)

$$D = (D'/L^2)L^2. \tag{7}$$

The obtained apparent diffusion coefficients *D* can be well represented by the Eq. 7 in Fig. 11. The fitting of the data by Eq. 7 yields  $D'/L'^2 = 1.33 \times 10^{-4} \text{ 1/s}$ . Therefore, the results of OH decrease with time during the in situ IR observation can be explained by the *m* layers model with a unit length of *L'* with a constant mono-dimensional diffusion coefficient *D'*.

Although the unit cell of muscovite does not include the layer without OH, the  $K^+$ -bearing interlayer might act as a kind of barrier layer corresponding to the above *m* layers

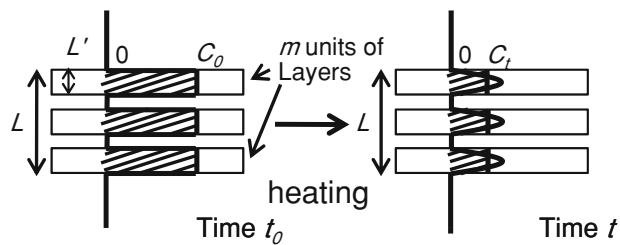


**Fig. 12** A Schematic model for the mono-dimensional diffusion for the *m* layers with a unit length of *L'* with a constant mono-dimensional diffusion coefficient *D'* with a total thickness of *L* and total initial concentration of *C*<sub>0</sub>. After a time *t*, the concentration decreases to *C*<sub>*t*</sub> by the diffusion. The *C*<sub>*t*</sub> value is indicated as rectangular areas which are equal to the areas under the diffusion profiles

model. If the unit length of *L'* is 1 nm (10 Å), which is the unit cell size of muscovite (Bailey 1984), *D'* becomes  $1.33 \times 10^{-22} \text{ m}^2/\text{s}$ . Kogure and Nespolo (1999) observed by TEM periodical units of 36 nm in [100] direction of biotite. By taking *L'* as 36 nm, *D'* becomes  $1.73 \times 10^{-19} \text{ m}^2/\text{s}$ . This is close to diffusion coefficients of oxygen in silicate tetrahedral networks such as in quartz and feldspars (Giletti and Yund 1984; Elphick et al. 1988) (Table 4; Fig. 13). Moreover, density of defects such as dislocations might also affect the unit length. For example, although no dislocation density data are found for muscovite, typical dislocation densities reported for olivine are about three dislocations per 1 μm sample thickness, and average unit length can be estimated to be in the order of 300 nm (Kitamura et al. 1987). By taking *L'* as 300 nm, *D'* becomes  $1.20 \times 10^{-17} \text{ m}^2/\text{s}$ . This is close to diffusion coefficients of <sup>18</sup>O in muscovite in the order of  $10^{-16} \text{ m}^2/\text{s}$ , determined by isotope exchange of <sup>18</sup>O (Fortier and Giletti 1991) (Table 4; Fig. 13). Although real unit length *L'* data for muscovite are required in the future, possibly by TEM observation of muscovite, the above evaluation indicates that the *m* layer mono-dimensional diffusion model might explain the observed experimental results of muscovite dehydration.

The diffusivity ranges for muscovite flakes estimated above are much smaller than that extrapolated from the reported values for muscovite powders (Fortier and Giletti 1991) (Fig. 13). The muscovite flakes used in this study are long enough in the perpendicular direction to *c* ( $\parallel c$ -axis:  $\perp c$ -axis = 10 μm:3 mm) to obtain slow diffusion in the parallel direction to *c* by the in situ observation in this direction. On the other hand, muscovite powders can be considered to be have similar length in both directions ( $\parallel c$ -axis:  $\perp c$ -axis = 1:1) and the diffusion process measured by the oxygen isotope exchange included large contributions from the faster diffusion perpendicular to *c* (Fortier and Giletti 1991). Therefore, their diffusion data

**Table 4** Summary of experimental data for oxygen diffusion in various materials

Mineral	Orientation	Temperature range (°C)	Pressure (MPa)	Activation energy (kJ/mol)	Log $D_0$ ( $\text{m}^2/\text{s}$ )	Reference
$\alpha$ -quartz	//c-axis	450–590	100	243	–16.4	Farver and Yund (1991)
$\beta$ -quartz	//c-axis	600–800	100	142	–17.3	Giletti and Yund (1984)
$\beta$ -quartz	$\perp$ c-axis	600–800	100	234	–19.4	Giletti and Yund (1984)
Anorthite	$\perp$ (001)	850–1300	0.1	236	–20.5	Elphick et al. (1988)
Muscovite	Powder	512–700	100	163	–16.1	Fortier and Giletti (1991)

The diffusion coefficients in these references were determined by isotope exchange of  $^{18}\text{O}$

for muscovite powders have much larger diffusivity and smaller activation energy (163 kJ/mol) than the present data on muscovite flakes (290 kJ/mol).

Mazzucato et al. (1999) studied muscovite dehydration by in situ high-temperature X-ray powder diffraction (XRPD) and the kinetic analysis using an Avrami-type model gave the mono-dimensional diffusion-limited mechanism with apparent activation energy of about 251 kJ/mol. They considered that the nucleation of dehydroxylated phase was followed by the growth of a high-temperature muscovite phase. The activation energy value for muscovite flakes in this study is similar and so the decrease of OH by mono-dimensional diffusion observed in this study might be followed by the nucleation and growth of a dehydroxylated high-temperature phase.

The activation energy value (290 kJ/mol) obtained in Fig. 9 for apparent diffusion coefficients  $D$  will not be changed for true values  $D'$  for different unit length  $L'$ . This value is much larger than that for  $^{18}\text{O}$  diffusion in muscovite (163 kJ/mol) (Fortier and Giletti 1991) but closer to those for  $^{18}\text{O}$  diffusion in anorthite (236 kJ/mol) (Elphick et al. 1988) and in  $\beta$ -quartz (234 kJ/mol) (Giletti and Yund 1984) (Fig. 13; Table 4). Therefore, the above dehydration process might be rate-limited by mono-dimensional diffusion through tetrahedral silicate sheet perpendicular to (001) planes of muscovite.

## Conclusions

In situ high-temperature IR microspectroscopy of muscovite were conducted for investigating dehydration mechanisms of muscovite flakes by directly observing detailed OH decrease in muscovite.

First, we observed the absorption band around  $3,620\text{ cm}^{-1}$  assigned to stretching vibration of OH at 760, 790, 800, 810, 820, 840 and  $860^\circ\text{C}$ . The intensity of the  $3,620\text{ cm}^{-1}$  band decreased with time, which indicated that OH in muscovite decreased during the dehydration experiments.

Second, the decrease curves were fitted by possible rate equations (the first order reaction; the second order

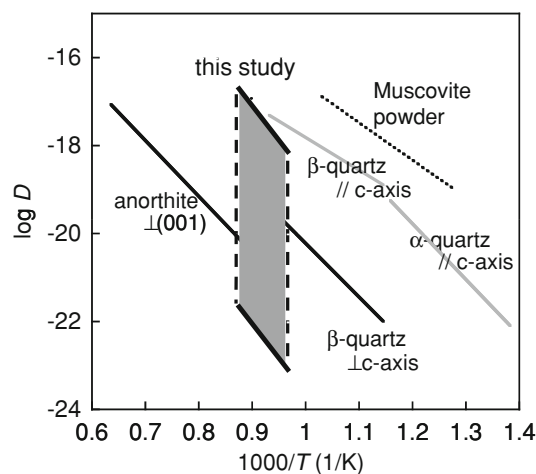


**Fig. 13** Arrhenius diagram of oxygen diffusivities for various silicates. Numerical values and references for these data are listed in Table 4. The mono-dimensional diffusion coefficients  $D'$  through a unit length of  $L'$  for muscovite flakes show activation energy of 290 kJ/mol and diffusion coefficients ranging from  $1.33 \times 10^{-22}$  to  $1.20 \times 10^{-17}\text{ m}^2/\text{s}$  for different unit lengths from 1 to 300 nm (shaded rhombic area)

reaction; the mono-dimensional diffusion; the two-dimensional diffusion) and the mono-dimensional diffusion was found to be the best fit among the rate laws tested at all the temperatures. The obtained diffusion coefficients were plotted in an Arrhenius diagram giving the activation energy of  $290 \pm 20\text{ kJ/mol}$ .

Third, muscovite flake samples with varying thickness from  $4.0$  to  $19.7\text{ }\mu\text{m}$  were measured by the in situ IR microspectroscopy at  $840^\circ\text{C}$ . The obtained apparent diffusion coefficients  $D$  changed with the sample thickness  $L$ . A mono-dimensional diffusion model within layers of a constant unit length  $L'$  stacking vertically until  $m$  layers separated by other layers without any OH (zero concentration) (Fig. 12) was considered to explain this  $D$  variation with  $L$ . Based on this  $m$  layers model with a unit length of  $L'$  with a constant mono-dimensional diffusion coefficient  $D'$ , the  $D$  variation with  $L$  can be well reproduced by the predicted relation:  $D = (D'/L'^2)L^2$ .

Therefore, the dehydration process might be rate-limited by mono-dimensional diffusion through tetrahedral silicate sheet perpendicular to (001) planes of muscovite.

**Acknowledgments** We are grateful to SII-NT for their kind assistance in thermogravimetry of the samples. We thank Ms. M. Yoshizaki of Tokyo Institute of Technology for her assistance of the EPMA analyses. We also thank Dr. M. Katsura, Mr. Y. Kirino and Dr. T. Yokoyama of Osaka University for their helpful supports in the data fitting procedures and constructive comments.

## References

- Abbott RN Jr (1994) Energy calculations bearing on the dehydroxylation of muscovite. *Can Mineral* 32:87–92
- Aines RD, Rossman GR (1985) The high temperature behavior of trace hydrous components in silicate minerals. *Am Mineral* 70:1169–1179
- Bailey SW (1984) Crystal chemistry of the true micas. In: Bailey SW (ed) *Micas. Reviews in Mineralogy*, vol 13. Mineralogical Society of America, pp 13–16
- Brindley GW, Brown G (1980) *Crystal structures of clay minerals and their X-ray identification*. Mineralogical Society, London
- Carlsaw HS, Jaeger JC (1959) *Conduction of heat in solids*, vol 2. Oxford University Press, London
- Eberhart JP (1963) Etude des transformations du mica muscovite par chauffage entre 700 et 1200°C. *Bull Soc Fr Minéral Cristallogr* 86:213–251
- Elphick SC, Graham CM, Dennis PF (1988) An ion microprobe study of anhydrous oxygen diffusion in anorthite: a comparison with hydrothermal data and some geological implications. *Contrib Mineral Petrol* 100:490–495. doi:10.1007/BF00371378
- Farver JR, Yund RA (1991) Oxygen diffusion in quartz: dependence on temperature and water fugacity. *Chem Geol* 90:55–70. doi:10.1016/0009-2541(91)90033-N
- Fortier SM, Giletti BJ (1991) Volume self-diffusion of oxygen in biotite, muscovite and phlogopite micas. *Geochim Cosmochim Acta* 55:1319–1330. doi:10.1016/0016-7037(91)90310-2
- Fyfe WS, Price NJ, Thompson AB (1978) *Fluids in the earth's crust*. Elsevier, Amsterdam
- Gaines GL Jr, Vedder W (1964) Dehydroxylation of muscovite. *Nature* 201:495. doi:10.1038/201495a0
- Giletti BJ, Yund RA (1984) Oxygen diffusion in quartz. *J Geophys Res* 89:4039–4046. doi:10.1029/JB089iB06p04039
- Gridi-Bennadji F, Blanchart P (2007) Dehydroxylation kinetic and exfoliation of large muscovite flakes. *J Therm Anal Calorim* 90:747–753. doi:10.1007/s10973-006-7888-4
- Guggenheim S, Chang Y-H, Koster van Groos AF (1987) Muscovite dehydration: high temperature studies. *Am Mineral* 72:537–550
- Hanykyr V, Ederova J, Travnicek Z, Srank J (1985) Isothermal dehydroxylation of muscovite mica. *Thermochim Acta* 93:517–520. doi:10.1016/0040-6031(85)85130-3
- Holt JB, Cutler IB, Wadsworth ME (1958) Rate of thermal dehydration of muscovite. *J Am Ceram Soc* 41:242–246. doi:10.1111/j.1151-2916.1958.tb13548.x
- Holt JB, Cutler IB, Wadsworth ME, Klein C, Hurlbut CS Jr (1964) Kinetics of the thermal dehydration of hydrous silicates. *Clays Clay Miner* 12:55–67. doi:10.1346/CCMN.1963.0120109
- Kitamura M, Kondoh S, Morimoto N, Miller GH, Rossman GR, Putnis A (1987) Planar OH-bearing defects in mantle olivine. *Nature* 328:143–145. doi:10.1038/328143a0
- Klein C, Hurlbut CS Jr (1993) *Manual of mineralogy*, 21st edition edn. Wiley and Sons, New York, pp 515–517 (after James D. Dana)
- Kodama H, Brydon JE (1968) Dehydration of microcrystalline muscovite. *Trans Faraday Soc* 63:3112–3119
- Kogure T, Nespolo M (1999) A TEM study of long-period mica polytypes: determination of the stacking sequence of oxybiotite by means of atomic resolution images and periodic intensity distribution (PID). *Acta Crystallogr B* 55:507–516. doi:10.1107/S0108768199003845
- Mazzucato E, Artioli G, Gualtieri A (1999) High temperature dehydroxylation of muscovite-2 M (1): a kinetic study by in situ XRPD. *Phys Chem Miner* 26:375–381. doi:10.1007/s002690050197
- Okumura S, Nakashima S (2004) Water diffusivity in rhyolitic glasses as determined by in situ IR spectroscopy. *Phys Chem Miner* 31:183–189. doi:10.1007/s00269-004-0383-1
- Okumura S, Nakashima S (2005) Molar absorptivities of OH and H<sub>2</sub>O in rhyolitic glass at room temperature and at 400–600°C. *Am Mineral* 90:441–447. doi:10.2138/am.2005.1740
- Okumura S, Nakashima S (2006) Water diffusion in basaltic to dacitic glasses. *Chem Geol* 227:70–82. doi:10.1016/j.chemgeo.2005.09.009
- Okumura S, Nakamura M, Nakashima S (2003) Determination of molar absorptivity of IR fundamental OH-stretching vibration in rhyolitic glasses. *Am Mineral* 88:1657–1662
- Rossman GR (1984) Spectroscopy of micas. In: Bailey SW (ed) *Micas. Reviews in Mineralogy*, vol 13. Mineral Society of America, Washington DC, pp 145–181
- Rouxhet PG (1970) Kinetics of dehydroxylation and of OH–OD exchange in macrocrystalline micas. *Am Mineral* 55:841–853
- Sabatier MG (1955) Les transformations du mica muscovite aux environs de 700°C. *Bull Groupe Fr Argiles* 6:35–39
- Shishelova TI, Metslk MS, Sokolov KY (1974) Changes in the IR spectra of micas on heating. *Appl Spectrosc* 20:784–786. doi:10.1007/BF00614158
- Toraya H (1981) Distortions of octahedra and octahedral sheets in 1 M micas and the relation to their stability. *Z Kristallogr* 144:42–52
- Udagawa S, Urabe K, Ikawa H, Katoo K, Hasu H (1973) The study on thermal transformations of muscovite by Weissenberg camera with high temperature apparatus. *J Clay Sci Soc Jpn* 13:131–138
- Udagawa S, Urabe K, Hasu H (1974) The crystal structure of muscovite dehydroxylate. *Jpn Assoc Miner Petrol Econ Geol* 69:381–389